Journal of the Nigerian Association of Mathematical Physics
Volume 52 (*July & Sept., 2019 Issue*), **pp99 – 114**

FULLY DEVELOPED MHD NATURAL CONVECTION FLOW IN A VERTICAL ANNULAR MICROCHANNEL IN THE PRESENCE OF HEAT GENERATING/ABSORBING FLUID: AN EXACT SOLUTION

BabatundeAina[1] and Sani Isa[2]

[1] Department of Mathematics, Federal University, Gashua, Yobe State, Nigeria.
[2]Department of Mathematics, Yobe State University, Damaturu, Yobe State, Nigeria.

Abstract

An analytical solution for fully developed MHD natural convection flow of viscous, incompressible, electrically conducting fluid in a vertical annular micro-channel in the presence of heat generating/absorbing fluid is presented. The velocity slip and temperature jump at the annular micro-channel surfaces are taken into account. Exact solution of momentum equation is derived separately in terms of Bessel's function of first and second kind for heat generating fluid and modified Bessel's function of first and second kind for heat absorbing fluid. The solutions obtained are graphically represented and the effects of governing parameters on velocity, temperature, volume flow rate and rate of heat transfer are investigated in detail. Result reveals that, as Hartmann number increase, there is a decrease in the fluid velocity as well as skin friction and increase in slip velocity for both heat generation and absorption.

Keywords: Heat Generation/Absorption Fluid; Hartmann Number; Annular Microchannel; Velocity Slip; Temperature Jump

Nomenclature

$B_0 =$ constant magnetic flux density $C_{\rho_0} =$ specific heat at constant pressure
$\ln =$ fluid- wall interaction parameter, β_t/β_v $g =$ gravitational acceleration
$J_n =$ Bessel function of first kind of order n $Y_n =$ Bessel function of second kind of order n
$I_n =$ modified Bessel function of first kind of order n $k =$ thermal conductivity
$K_n =$ modified Bessel function of second kind of order n
$k_1 =$ radius of the inner cylinder $k_2 =$ radius of the outer cylinder
$Kn =$ Knudsen number, λ/w $M =$ Hartmann number
$q =$ volume flow rate $Q_m =$ dimensionless volume flow rate
$Q_0 =$ dimensional heat generation/absorption parameter $\Pr =$ Prandtl number
$r =$ dimensional radial coordinate $R =$ dimensionless radial coordinate
$\hat{R} =$ specific gas constant
$S =$ dimensionless heat generation/absorption parameter
$T =$ temperature of fluid $T_0 =$ reference temperature
$T_1 =$ temperature at outer surface of the inner cylinder $u =$ axial velocity
$U =$ dimensionless axial velocity $w =$ dimensional gap between the cylinders
$\sigma_t, \sigma_v =$ thermal and tangential momentum accommodation coefficients, respectively
$\alpha =$ thermal diffusivity $\beta_0 =$ coefficient of thermal expansion
$\beta_t, \beta_v =$ dimensionless variables $\gamma =$ ratio of specific heats

Corresponding Author**:** Babatunde A., Email: ainavicdydx@gmail.com, Tel: +2348063178775, +2348064743126 (SI)

$\mu_0 =$ dynamic viscosity $\theta =$ dimensionless temperature

$\rho_0 =$ density $\nu =$ fluid kinematic viscosity (μ_0/ρ_0)

$\eta =$ ratio of radii (k_1/k_2) $\lambda =$ molecular mean free path

$\sigma =$ electrical conductivity of the fluid $\tau =$ skin-friction

1. Introduction

Microflow has been given great importance in recent research activities due to its new application in microfluidic system devices, such as biomedical sample injection, biochemical cell reaction, microelectric ship cooling e.t.c. a fundamental understanding of the flow and thermal fields as well as the corresponding characteristics at microscale, which may deviate from those at macroscale, is required for the technological demands. Gaseous flow in microscale devices have been in the vanguard of research activities and have received great deal of attentions in recent years, due to the rapid growth of application in micrototal analysis systems and micro-electro- mechanical-systems (MEMS). These applications have raised the interest in understanding the physical aspects of fluid flow and convective heat transfer in both forced and natural forms through micron sized channels, known as micro-channels. There are many studies that have been conducted in the field of micro geometry flow. For instance, Chen and Weng [1] obtained exact solution of the fully developed natural convection in an open-ended vertical parallel-plate microchannel with asymmetric wall temperature distributions. The effects of rarefaction and fluid-wall interaction were shown to enhance the volume flow rate and to reduce the rate of heat transfer. This result is further extended by taking into account suction/injection on the microchannel walls by Jha *et al*. [2]. Their results showed that skin-friction as well as rate of heat transfer strongly depends on the suction/injection parameter. Numerical solutions were obtained by Buonomo and Manca [3] for natural convection in parallel-plate vertical microchannels due to asymmetric heating by imposing constant heat flux on the boundaries. The same authors [4] further performed a numerical study on transient mixed convection in a vertical microchannel that is asymmetrically or symmetrically heated at uniform heat fluxes. The transient hydrodynamics and thermal behaviours of fluid flow in an open-ended vertical parallel-plate microhannel, under the effect of the hyperbolic-heat-conduction model, were investigated semi-analytically in [5]. In recent past, the work of Chen and Weng [1]was extended to mixed convection by Avci and Adyin [6]. Avci and Aydin [7] conducted a study on fully developed mixed convective flowin a vertical micro-annulus formed by two concentric micro-tubes. Jha and Aina [8] further extended the work of Avci and Aydin [7] to the case when the vertical micro-annulus formed by two concentric micro-tubes are porous, i.e. where there is suction or injection through the annulus surfaces. They concluded in their study that as suction/injection on the micro-porous-annulus (MPA) increases, the fluid velocity and temperature increase. Also, Weng and Chen [9] studied the impact of wall surface curvature on natural convection flow in an open-ended vertical micro annulus with asymmetric heating of annulus surfaces. Recently, Jha *et al.* [10] further extended the work of Weng and Chen [9] by taking into account suction/injection on vertical annular micro-channel. They pointed out that skin-friction decrease at the outer surface of inner porous cylinder with increase of fluid- wall interaction parameter in case of injection at outer surface of the inner porous cylinder and simultaneous suction at inner surface of the outer porous cylinder while the result is just reverse at the inner surface of outer porous cylinder.

On the other hand, magnetohydrodynamic free convective flows along with the effects of heat and mass transfer have considerable applications in geophysics, metallurgy and engineering and science such as MHD pumps, MHD generators, magnetic suppression of molten semi conducting materials, MHD couples and bearings and magnetic control of molten iron flow in steel industry etc. Despite the fact that there are numerous studies on natural convection flow of an electrically conducting fluid in channels, there are just a few studies regarding natural convection flow of an electrically conducting fluid in microchannel. For example, Jha *et al.* [11] studied the fully developed steady natural convection flow of conducting fluid in a vertical parallel plate microchannel in the presence of transverse magnetic field. They found that, the increase of Hartmann number is responsible for decrease in the volume flow rate. The combined impact of transverse magnetic field and suction/injection on steady natural convection flow of conducting fluid in a vertical microchannel was carried out by Jha *et al.* [12]. The study reports that as suction/injection, rarefaction and fluid-wall interaction increase, the volume flow rate increases while it decreases with increase in Hartmann number. In another work, Jha *et al.* [13] investigated the role of wall surface curvature on transient MHD free convective flow in vertical micro-concentric-annuli. Their results showed that the slip induced by rarefaction effect and Hartmann number increases as radius ratio increases while the slip induced by fluid–wall interaction parameter increases as radius ratio decreases. Jha *et al.* [14] studied exact solution of steady fully developed natural convection flow of viscous, incompressible, and electrically conducting fluid in a vertical annular microchannel. They reported that increase in curvature radius ratio leads to an increase in the volume flow rate. Also, Jha and Aina [15] presented the MHD natural convection flow in a vertical micro-porous-annulus (MPA) in the presence of radial magnetic field. The MHD natural convection flow in vertical micro-concentric-annuli (MCA) in the presence of radial magnetic field has been discussed by Jha *et al*. [16]. They discovered that the skin friction decreases as Hartmann number increases. In another related work, Sheikholeslami *et al*. [17] studied the effect of magnetic field on nanofluid flow and heat transfer in a semi-annulus enclosure via control volume based finite element method. Khan and Ellahi [18] investigated the effects of magnetic field and porous medium on some unidirectional flows of a second grade fluid. Farhad *et al*. [19] conducted a study on the effects of slip condition on the unsteady magnetohydrodynamics (MHD) flow of incompressible visscoelasstic fluids in a porous channel under the influence of transverse magnetic field.

The study of heat generation/absorption effects in moving fluids is importance in view of several physical problems such as those dealing with chemical reactions and those concerned with dissociating fluids. A lot of interests have been built in the study of flow of heat generating/absorbing fluid because as the temperature differences are increased appreciably, the volumetric heat generation/absorption term may employ strong influence on the heat transfer and transitively on the flow [20]. Internal heat generation/absorption plays significant role in various physical phenomena such as convection in earth's mantle [21], application in the field of nuclear energy [22], post accident heat removal [23], fire and combustion modelling [24], and the development of metal waster from spent nuclear fuel [25]. Chamkha [26] considered non-Darcy fully developed mixed convection flow in a channel embedded in a porous medium in the presence of heat generation/absorption and hydromagnetic effects. Meanwhile, different attributes have been accorded internal heat generation/absorption: for instance, it was assumed to be constant in the study conducted by Inman [27], Ostrach [28], but considered as a function of space by Low [29], Chambre [30] and Toor [31]. In the works of Gee and Lyon [32], Modejski [33] and Toor [34], heat generation is taken to be frictional heating and expansion effects of the working fluid, while Moalem [35] presented heat generation as an inversely proportional value to $(a+bT)$. In addition, Foraboschi and Federico [36] presented the volumetric rate of heat generation/absorption which is directly proportional to $(T-T_0)$ and explained that it is an approximation of the state of some exothermic process with T_0 as the initial temperature. Recently, Jha *et al.* [37] analysed the influence of heat generating/absorbing fluid on fully developed mixed convection flow in a vertical micro-concentric-annulus (MCA) taking into account the velocity slip and temperature jump at the outer surface of inner cylinder and inner surface of outer cylinder.

The purpose of the present work is to present exact solutions for the mathematical model responsible for fully developed steady fully developed natural convection flow in a vertical annular microchannel in the presence of heat generation/absorption. The mathematical model employed herein represents a generalization of the work discussed by Jha*et al*.[14] by incorporating the effect of generating/absorbing fluid.

2. Mathematical Analysis

The geometry of the system under consideration in this present study is shown schematically in Figure 1. Let's considera steady laminar steady fully developed MHD natural convection flow in a vertical annular microchannel in the presence of heat generating/absorbing fluid. The $Z-$ axis is taken along the axis of the cylinders in the vertical upward direction while the $r-$ axis is in the radial direction. The radius of the inner cylinder and outer cylinder is k_1 and k_2 respectively. The flow is assumed to be fully developed both hydrodynamically and thermally. The viscous dissipation and compressibility effects in the fluid radiation effects are neglected. A magnetic field of uniform strength B_0 is assumed to be applied in the direction perpendicular to the direction of flow. It is assumed that the magnetic Reynolds number is very small, which corresponds to negligibly induced magnetic field compared to the externally applied one [38].Since the flow is fully developed and cylinders are of infinite length, the flow depends only on radial coordinate (r). The mathematical model used in the present work to capture the heat generation/absorptioninside the fluid is [36]

$$Q=Q_0(T-T_0) \tag{1}$$

The mathematical model employed herein represents a generalization of the work discussed by Jha et al.[14] to include the role of heat generating/absorbing fluid on fully developed natural convection flow in a vertical annular microchannel. By using Boussinesq's approximation, the governing equations for momentum and energy can be written in dimensional form as follows:

Conservation of momentum [14]

$$\frac{\nu}{r}\frac{d}{dr}\left(r\frac{du}{dr}\right)+g\beta_0(T-T_0)-\frac{\sigma B_0^2 u}{\rho_0}=0 \tag{2}$$

Conservation of energy

$$\frac{\alpha}{r}\frac{d}{dr}\left(r\frac{dT}{dr}\right)\pm\frac{Q_0}{\rho_0 C_\rho}(T-T_0)=0 \tag{3}$$

The boundary conditions for the velocity and temperature field in the presence of velocity slip and temperature jump are [14]:

$$u(r=k_1)=\frac{2-\sigma_v}{\sigma_v}\lambda\left.\frac{du}{dr}\right|_{r=k_1} \tag{4}$$

$$u(r=k_2)=-\frac{2-\sigma_v}{\sigma_v}\lambda\frac{du}{dr}\bigg|_{r=k_2} \qquad (5)$$

$$T(r=k_1)=T_1+\frac{2-\sigma_t}{\sigma_t}\frac{2\gamma}{\gamma+1}\frac{\lambda}{\Pr}\frac{dT}{dr}\bigg|_{r=k_1} \qquad (6)$$

$$T(r=k_2)=T_0-\frac{2-\sigma_t}{\sigma_t}\frac{2\gamma}{\gamma+1}\frac{\lambda}{\Pr}\frac{dT}{dr}\bigg|_{r=k_2} \qquad (7)$$

By introducing the following non-dimensional quantities

$$R=\frac{r-k_1}{w},\ w=k_2-k_1,\ U=\frac{u}{u_c},\ \theta=\frac{T-T_0}{T_1-T_0},\ u_c=\frac{\rho_0 g\beta_0(T_1-T_0)w^2}{\mu_0},\ \Pr=\frac{C_{\rho_0}\mu_0}{k_0},\ Kn=\frac{\lambda}{w},$$

$$\beta_v=\frac{2-\sigma_v}{\sigma_v},\ \beta_t=\frac{2-\sigma_t}{\sigma_t}\frac{2\gamma}{\gamma+1}\frac{1}{\Pr},\ \lambda=\frac{\sqrt{\pi\hat{R}T_0/2\mu_0}}{\rho_0},\ S^2=\frac{Q_0w^2}{k_0},\ \ln=\frac{\beta_t}{\beta_v},\ \eta=\frac{k_1}{k_2},\ M^2=\frac{\sigma B_0^2w^2}{\rho_0\nu} \qquad (8)$$

Using equation (8) in equations (1-7), the dimensionless form of momentum and energy equations are:

$$\frac{1}{[\eta+(1-\eta)R]}\frac{d}{dR}\left[[\eta+(1-\eta)R]\frac{dU}{dR}\right]-M^2U+\theta=0 \qquad (9)$$

$$\frac{1}{[\eta+(1-\eta)R]}\frac{d}{dR}\left[[\eta+(1-\eta)R]\frac{d\theta}{dR}\right]\pm S^2\theta=0 \qquad (10)$$

The boundary conditions which describe velocity slip and temperature jump conditions at the fluid – wall interface in dimensionless form are [9]:

$$U(0)=\beta_v Kn\frac{dU}{dR}\bigg|_{R=0},\ U(1)=-\beta_v Kn\frac{dU}{dR}\bigg|_{R=1} \qquad (11)$$

$$\theta(0)=1+\beta_v Kn\ln\frac{d\theta}{dR}\bigg|_{R=0},\ \theta(1)=-\beta_v Kn\ln\frac{d\theta}{dR}\bigg|_{R=1} \qquad (12)$$

The physical quantities used in the above equations are defined in the nomenclature.
By using the transformation $Z=\eta+(1-\eta)R$, the equations (8) to (11) can be written as:

$$\frac{1}{Z}\frac{d}{dZ}\left[Z\frac{dU}{dZ}\right]-\frac{M^2U}{(1-\eta)^2}+\frac{\theta}{(1-\eta)^2}=0 \qquad (13)$$

$$\frac{1}{Z}\frac{d}{dZ}\left[Z\frac{d\theta}{dZ}\right]\pm\frac{S^2\theta}{(1-\eta)^2}=0 \qquad (14)$$

Subject to the boundary conditions

$$U(\eta)=\beta_v Kn(1-\eta)\frac{dU}{dZ}\bigg|_{Z=\eta},\qquad U(1)=-\beta_v Kn(1-\eta)\frac{dU}{dZ}\bigg|_{Z=1} \qquad (15)$$

$$\theta(\eta)=1+\beta_v Kn\ln(1-\eta)\frac{d\theta}{dZ}\bigg|_{Z=\eta},\qquad \theta(1)=-\beta_v Kn\ln(1-\eta)\frac{d\theta}{dZ}\bigg|_{Z=1} \qquad (16)$$

It should be mentioned that the form of the analytical solutions for temperature are different for a heat generating (positive sign in equation (14)) and heat absorbing fluid (negative sign in equation (14)). Closed form solutions are derived for these two cases separately.

CASE 1: HEAT - GENERATING FLUID

For this type of fluid the energy equation (equation (14)) with the positive sign in the second term is a differential equation that has the following closed form solution for temperature:

$$\theta(Z)=C_1J_0(E_1Z)+C_2Y_0(E_1Z) \qquad (17)$$

where C_1 and C_2 are arbitrary constants determined by the boundary condition given in equation (16). Using the boundary conditions, C_1 and C_2 becomes

$$C_1=-\frac{E_5}{[E_3E_4-E_2E_5]}\ \text{and}\ C_2=\frac{E_4}{[E_3E_4-E_2E_5]} \qquad (18)$$

with the solution for temperature already determined, equation (13) can be solved for velocity (U), subjected to the boundary conditions given in equation (15). The general solution of equation (13) after substitution equation (17) in equation (13) is obtained by rearranging the homogeneous part to take the general form of the Bessel equation [39]. The particular solution of equation (13) is sought by assuming an appropriate form (according to the forcing function i.e., the right hand side of equation (13)).The exact solution of equation (13)under the appropriate velocity slip condition defined in equation (15)is

$$U(Z) = C_5 I_0(F_1 Z) + C_6 K_0(F_1 Z) + \frac{1}{[M^2 - S^2]}[C_1 J_0(E_1 Z) + C_2 Y_0(E_1 Z)] \tag{19}$$

In above equation, the constants C_5 and C_6 are

$$C_5 = \frac{F_3F_7 - F_4F_6}{F_3F_5 - F_2F_6} \text{ and } C_6 = \frac{F_4F_5 - F_2F_7}{F_3F_5 - F_2F_6} \tag{20}$$

Three important parameters for convective micro-flow are the volume flow rate, skin – friction and rate of heat transfer. The dimensionless volume flow rate is:

$$Q_m = \frac{q}{2\pi w^2 u_c} = \frac{1}{(1-\eta)^2}\int_\eta^1 ZU(Z)dZ \tag{21}$$

Substituting equation (19) into equation (21), one obtain

$$Q_m = \frac{1}{(1-\eta)^2}\left[\begin{array}{l} \frac{1}{F_1}\{(C_5 I_1(F_1) - C_5\eta I_1(F_1\eta)) + (C_6 K_1(F_1) - C_6\eta K_1(F_1\eta))\} \\ + \frac{1}{E_1[M^2 - S^2]}\{(C_1 J_1(E_1) - C_1\eta J_1(E_1\eta)) + (C_2 Y_1(E_1) - C_2\eta Y_1(E_1\eta))\} \end{array}\right] \tag{22}$$

The skin - frictions (τ) at the cylinder walls are obtained by differentiating the velocity (equation (19)) as follows:

$$\tau_0 = \left.\frac{dU}{dR}\right|_{R=0} = (1-\eta)\left.\frac{dU}{dZ}\right|_{Z=\eta} \tag{23}$$

$$\tau_0 = (1-\eta)\left[F_1\{(C_5 I_1(F_1\eta) - C_6 K_1(F_1\eta))\} + \frac{E_1}{[S^2 - M^2]}\{(C_1 J_1(E_1\eta) + C_2 Y_1(E_1\eta))\}\right] \tag{24}$$

$$\tau_1 = \left.\frac{dU}{dR}\right|_{R=1} = (1-\eta)\left.\frac{dU}{dZ}\right|_{Z=1} \tag{25}$$

$$\tau_0 = (1-\eta)\left[F_1\{(C_5 I_1(F_1) - C_6 K_1(F_1))\} + \frac{E_1}{[S^2 - M^2]}\{(C_1 J_1(E_1) + C_2 Y_1(E_1))\}\right] \tag{26}$$

Also, the rate of heat transfer (Nu) at the cylinder walls are obtained by differentiating the temperature (equation (17)) as follows:

$$Nu_0 = -\left.\frac{d\theta}{dR}\right|_{R=0} = -(1-\eta)\left.\frac{d\theta}{dZ}\right|_{Z=\eta} \tag{27}$$

$$Nu_0 = S[C_1 J_1(E_1\eta) + C_2 Y_1(E_1\eta)] \tag{28}$$

$$Nu_1 = -\left.\frac{d\theta}{dR}\right|_{R=1} = -(1-\eta)\left.\frac{d\theta}{dZ}\right|_{Z=1} \tag{29}$$

$$Nu_1 = S[C_1 J_1(E_1) + C_2 Y_1(E_1)] \tag{30}$$

It should be mentioned that in the absence of the fluid heat generation effect, equations (17)–(30) are consistent with those reported by Weng and Chen [9]

CASE 2: HEAT –ABSORBING FLUID

For this type of fluid, the energy equation (equation (14)) with the negative sign in the second term is a differential equation that has the following closed form solution for temperature:

$$\theta(Z) = C_3 I_0(E_1 Z) + C_4 K_0(E_1 Z) \tag{31}$$

where C_3 and C_4 are arbitrary constants determined by the boundary condition given in equation (16). Using the boundary conditions, C_3 and C_4 becomes

$$C_3 = -\frac{E_{10}}{[E_8E_9 - E_7E_{10}]} \text{ and } C_4 = \frac{E_9}{[E_8E_9 - E_7E_{10}]} \tag{32}$$

with the solution for temperature already determined, equation (13) can be solved for velocity (U), subjected to the boundary conditions given in equation (15). The general solution of equation (13) after substitution equation (31) in equation (13) is obtained by rearranging the homogeneous part to take the general form of the Bessel equation [39]. The particular solution of equation (13) is sought by assuming an appropriate form (according to the forcing function i.e., the right hand side of equation (13)).The exact solution of equation (13) under the appropriate velocity slip condition defined in equation (15) is

$$U(Z)=C_7I_0(F_1Z)+C_8K_0(F_1Z)+\frac{1}{[M^2-S^2]}[C_3I_0(E_1Z)+C_4K_0(E_1Z)] \tag{33}$$

where

$$C_7=\frac{F_9F_{13}-F_{10}F_{12}}{F_9F_{11}-F_8F_{12}} \text{ and } C_8=\frac{F_{10}F_{11}-F_{13}F_8}{F_9F_{11}-F_8F_{12}} \tag{34}$$

The dimensionless volume flow rate is:

$$Q_m=\frac{q}{2\pi w^2u_c}=\frac{1}{(1-\eta)^2}\int_\eta^1 ZU(Z)dZ \tag{35}$$

Substituting equation (33) into equation (35), one obtain

$$Q_m=\frac{1}{(1-\eta)^2}\left[\begin{array}{l}\frac{1}{F_1}\{(C_7I_1(F_1)-C_7\eta I_1(F_1\eta))-(C_8K_1(F_1)-C_8\eta K_1(F_1\eta))\}\\ +\frac{1}{E_1[M^2-S^2]}\{(C_3I_1(E_1)-C_3\eta I_1(E_1\eta))-(C_4K_1(E_1)-C_4\eta K_1(E_1\eta))\}\end{array}\right] \tag{36}$$

The skin - frictions (τ) at the cylinder walls are obtained by differentiating the velocity (equation (33)) as follows:

$$\tau_0=\left.\frac{dU}{dR}\right|_{R=0}=(1-\eta)\left.\frac{dU}{dZ}\right|_{Z=\eta} \tag{37}$$

$$\tau_0=(1-\eta)\left[F_1\{(C_7I_1(F_1\eta)-C_8K_1(F_1\eta))\}+\frac{E_1}{[M^2-S^2]}\{(C_3I_1(E_1\eta)-C_4K_1(E_1\eta))\}\right] \tag{38}$$

$$\tau_1=\left.\frac{dU}{dR}\right|_{R=1}=(1-\eta)\left.\frac{dU}{dZ}\right|_{Z=1} \tag{39}$$

$$\tau_1=(1-\eta)\left[F_1\{(C_7I_1(F_1)-C_8K_1(F_1))\}+\frac{E_1}{[M^2-S^2]}\{(C_3I_1(E_1)-C_4K_1(E_1))\}\right] \tag{40}$$

Also, the rate of heat transfer (Nu) at the cylinder walls are obtained by differentiating the temperature (equation (31)) as follows:

$$Nu_0=-\left.\frac{d\theta}{dR}\right|_{R=0}=-(1-\eta)\left.\frac{d\theta}{dZ}\right|_{Z=\eta} \tag{41}$$

$$Nu_0=-S[C_3I_1(E_1\eta)-C_4K_1(E_1\eta)] \tag{42}$$

$$Nu_1=-\left.\frac{d\theta}{dR}\right|_{R=1}=-(1-\eta)\left.\frac{d\theta}{dZ}\right|_{Z=1} \tag{43}$$

$$Nu_1=-S[C_3I_1(E_1)-C_4K_1(E_1)] \tag{44}$$

where $F_1,...,F_{13}$ are all constants given in the Appendix

3. RESULTS AND DISCUSSION

The solutions obtained above are functions of the governing non-dimensional parameters: the heat generation/absorption parameter (S), Hartmann number (M), radius ratio (η), rarefaction parameter $(\beta_v Kn)$, and fluid-wall interaction parameter $(\ln)$. Their influences on the velocity, temperature, volume flow rate, skin friction and rate of heat transfer are discussed here. The present parametric study has been performed in the continuum and slip flow regimes $(Kn \le 0.1)$. This study has been performed over the reasonable ranges of $0 \le \beta_v Kn \le 0.1$ and $0 \le \ln \le 10$. The selected reference values of $\beta_v Kn$, and $\ln$ for the present analysis are 0.05 and 1.64 respectively as given in Weng and Chen [9].

Figures 2 and 3 display the thermal response of the fluid to variation in rarefaction parameter $(\beta_v Kn)$ and fluid – wall interaction parameter $(\ln)$.It is observed that for both heat generation and absorption, the increase in rarefaction parameter as well as fluid-wall interaction parameter leads to an increase in the temperature jump on the outer surface of the inner cylinder as well as inner surface of outer cylinder. This is due to the reduction in the interaction between the fluid molecules and the heated boundary. It is interesting to note that, there exist points of inflection inside the vertical annular microchanel where temperature field is independent of both rarefaction parameter as well as the fluid - wall interaction parameter and also, the location of point of inflection is strongly dependent on curvature radius ratio (η).

Figures 4 and 5 illustrate the effects of rarefaction parameter $(\beta_v Kn)$as well as fluid-wall interaction parameter $(\ln)$ on velocity profile. In Figure 4, it is observed that for both heat generation and heat absorption, as rarefaction parameter increases, the velocity slip at the boundary increases which reduces the retarding effect of the boundary. This yields an observable increase in the fluid velocity. Furthermore, as rarefaction parameter increases, the temperature jump increases and reduces the amount of heat transfer from the boundary to the fluid. This reduction in heat transfer reduces the buoyancy effect, which derives the flow and hence reduces the fluid velocity far from the boundary. It is evident from Figure 5 that, increase in fluid – wall interaction parameter $(\ln)$ leads to decrease in fluid velocity for both heat generation and absorption. Furthermore, by increasing curvature radius ratio (η) increases the velocity slip.

Figures 6 and 7 exhibit the effects of the heat generation/absorption parameter (S) on the temperature and velocity, respectively. It is seen that, temperature and velocity is a decreasing function of heat absorption parameter while increasing function of heat generation parameter. This is physically true because heat generation causes temperature distribution to increase, while on the contrary, heat absorption decreases the temperature distribution. In addition, increasing curvature radius ratio (η), increases the temperature jump and velocity slip.

Figure 8 depicts the velocity distribution for different values of Hartmann number (M). It is observed for both heat generation and absorption that as Hartmann number (M) increases, there is decrease in the fluid velocity and increase in slip velocity. This is physically true because, the application of magnetic field creates a resistive force similar to the drag force that acts in the opposite direction of the fluid motion, thus causing the fluid velocity to decreases. It is also observed that there is higher slip at inner surface of outer cylinder compare to outer surface of inner cylinder. In addition, for fixed Hartmann number (M), as radius ratio (η) increases there is an increase in the slip.

Figure 9show the effects of rarefaction parameter $(\beta_v Kn)$ and fluid-wall interaction parameter $(\ln)$ on the volume flow rate (Q_m). It is clear from Figure 9 that the volume flow rate (Q_m) is a decreasing function of fluid-wall interaction parameter $(\ln)$ for both heat generation and absorption. In addition, it is evident from the Figure also that, increasing the values of radius ratio and rarefaction parameter causes enhancement in the volume flow rate.

Figures 10 exhibit the effects of heat generation/absorption parameter (S) as well as rarefaction parameter $(\beta_v Kn)$ on the volume flow rate (Q_m). It is observed that, the volume flow rate (Q_m) increases with increase in heat generation parameter while it decreases with increase in heat absorption parameter. In addition, increase in rarefaction parameter $(\beta_v Kn)$ and radius ratio (η) leads to increase in the volume flow rate.

Figure 11 illustrate the effect of rarefaction parameter $(\beta_v Kn)$ and Hartmann number (M) on the volume flow rate (Q). It is found for both heat generation and absorption that, the volume flow rate (Q) decreases as Hartmann number (M) increases. Furthermore, increasing the value of rarefaction parameter $(\beta_v Kn)$ leads to increase in the volume flow rate.

Figures 12 exhibit the effects of fluid – wall interaction parameter $(\ln)$ as well as rarefaction parameter $(\beta_v Kn)$ on the skin-friction at outer surface of inner cylinder $(R=0)$.The skin - friction was observed to decrease with the increase in the fluid – wall interaction parameter $(\ln)$ as well as rarefaction parameter $(\beta_v Kn)$ for both heat generation and absorption.

Figures13 illustrate the effects of fluid – wall interaction parameter $(\ln)$ and rarefaction parameter $(\beta_v Kn)$ on the skin-friction at inner surface of outer cylinder $(R=1)$. It is obvious for both heat generation and absorption that increase in radius ratio (η) and rarefaction parameter $(\beta_v Kn)$ leads to the increase in the skin-friction.

Figures 14 and 15 exhibit the effects of heat generation/absorption parameter (S) and rarefaction parameter $(\beta_v Kn)$ on the skin-friction at outer surface of inner cylinder $(R=0)$ and inner surface of outer cylinder $(R=1)$, respectively. It is found from Figures 14a and 15a that the skin friction increases with increase in heat generation parameter at outer surface of inner cylinder $(R=0)$ and inner surface of outer cylinder $(R=1)$ while the reverse trend is observed in the case of heat absorption parameter as shown in 14b and 15b

Figures 16 and 17 depicts the variation of skin-friction at outer surface of inner cylinder $(R=0)$ and inner surface of outer cylinder $(R=1)$, respectively for different values of Hartmann number (M). It is evident from these Figures that for both heat generation and absorption, skin friction decreases as Hartmann number (M) increases.

The rate of heat transfer at outer surface of inner cylinder $(R=0)$ and inner surface of outer cylinder $(R=1)$ for different values of fluid – wall interaction parameter $(\ln)$ are shown in Figures 18 and 19 respectively. It is clear that the rate of heat transfer decreases with the increase of rarefaction parameter $(\beta_v Kn)$ and fluid – wall interaction parameter (ln) for both heat generation and absorption. Furthermore, it is worthy to note that as the value of curvature radius ratio (η) decreases, rate of heat transfer increases.

Figures 20 and 21 illustrate the effects of heat generation/absorption parameter (S) and rarefaction parameter $(\beta_v Kn)$ on the rate of heat transfer at outer surface of inner cylinder $(R=0)$ and inner surface of outer cylinder $(R=1)$ respectively. It is concluded that the rate of heat transfer increases with increase in heat generation parameter at outer surface of inner cylinder $(R=0)$ and inner surface of outer cylinder $(R=1)$ while the reverse trend is noticed in the case of heat absorption parameter.

In order to verify the accuracy of the present work, we have computed the numerical value for the velocity for small value of M and S. Table 1 gives a comparison of the numerical values of the velocity obtained in the present work when S and $M \to 0$ with those obtained by Weng and Chen [9] for $\ln = 1.64$ while Table 2 gives a comparison of the numerical values of the temperature obtained in the present work when $S \to 0$ with those obtained by Weng and Chen [9] for $\ln = 1.64$. As can be seen from Tables 1 and 2, the solutions of the present work perfectly agree with those of Weng and Chen [9].

CONCLUSION

The impact of heat generating/absorbing fluid on fully developed steady natural convection flow of viscous, incompressible, electrically conducting fluid in vertical annular microchannel in the presence of transverse magnetic field is analysed. The solution of velocity, temperature, volume flow rate, skin friction and rate of heat transfer is obtained in terms of heat generating/absorbing parameter (S), radius ratio (η), Hartmann number (M), rarefaction parameter $(\beta_v Kn)$, and fluid-wall interaction parameter $(\ln)$ on the temperature, velocity, volume flow rate, skin-friction and rate of heat transfer. This study exactly agrees with the finding of Chen and Weng [9] in the absence of transverse magnetic field and heat generating/absorbing fluid. From the indicated results of the present problem, the following conclusions are made:

I. It is found that temperature and velocity are decreasing function of heat absorption parameter while increasing function of heat generation parameter.
II. As Hartmann number (M) increases, there is a decrease in the fluid velocity as well as skin friction and increase in slip velocity for both heat generation and absorption.
III. The volume flow rate (Q_m) increases with increase in heat generation parameter while it decreases with increase in heat absorption parameter.
IV. The increase in Hartmann number (M) leads to decrease in the volume flow rate for both heat generation and absorption.
V. Skin friction increases with increase in heat generation parameter at outer surface of inner cylinder $(R=0)$ and inner surface of outer cylinder $(R=1)$ while the reverse trend is observed in the case of heat absorption parameter.
VI. Finally, the rate of heat transfer increases with increase of heat generation parameter at outer surface of inner cylinder $(R=0)$ and inner surface of outer cylinder $(R=1)$ while the reverse trend in the case of heat absorption parameter.

APPENDIX

Constants used in the present work.

$$E_1 = \frac{S}{(1-\eta)},\ E_2 = [J_0(E_1\eta) + \beta_v Kn \ln S J_1(E_1\eta)],\ E_3 = [Y_0(E_1\eta) + \beta_v Kn \ln S Y_1(E_1\eta)],$$

$$E_4 = [J_0(E_1) - \beta_v Kn \ln S J_1(E_1)],\ E_5 = [Y_0(E_1) - \beta_v Kn \ln S Y_1(E_1)],\ E_7 = [I_0(E_1\eta) - \beta_v Kn \ln S I_1(E_1\eta)],$$

$$E_8 = [K_0(E_1\eta) + \beta_v Kn \ln S K_1(E_1\eta)],\ E_9 = [I_0(E_1) + \beta_v Kn \ln S I_1(E_1)],\ E_{10} = [K_0(E_1) - \beta_v Kn \ln S K_1(E_1)],\ F_1 = \frac{M}{(1-\eta)},$$

$$F_2 = [I_0(F_1\eta) - \beta_v Kn(1-\eta)F_1 I_1(F_1\eta)],\ F_3 = [K_0(F_1\eta) + \beta_v Kn(1-\eta)F_1 K_1(F_1\eta)],$$

$$F_4 = \frac{1}{[S^2 - M^2]}[C_1 J_0(E_1\eta) + C_2 Y_0(E_1\eta) + \beta_v Kn(1-\eta)E_1\{C_1 J_0(E_1\eta) + C_2 Y_0(E_1\eta)\}],$$

$$F_5 = [I_0(F_1) + \beta_v Kn(1-\eta)F_1 I_1(F_1)],\ F_6 = [K_0(F_1) - \beta_v Kn(1-\eta)F_1 K_1(F_1)],$$

$$F_7 = \frac{1}{[S^2 - M^2]}[C_1 J_0(E_1) + C_2 Y_0(E_1\eta) - \beta_v Kn(1-\eta)E_1\{C_1 J_0(E_1) + C_2 Y_0(E_1)\}],$$

$$F_8 = [I_0(F_1\eta) - \beta_v Kn(1-\eta)F_1 I_1(F_1\eta)],\ F_9 = [K_0(F_1\eta) + \beta_v Kn(1-\eta)F_1 K_1(F_1\eta)],$$

$$F_{10} = \frac{1}{[M^2 - S^2]}[\beta_v Kn(1-\eta)E_1\{C_3 I_1(E_1\eta) - C_4 K_1(E_1\eta)\} - \{C_3 I_0(E_1\eta) + C_4 K_0(E_1\eta)\}],$$

$$F_{11} = [I_0(F_1) + \beta_v Kn(1-\eta)F_1 I_1(F_1)],\ F_{12} = [K_0(F_1) - \beta_v Kn(1-\eta)F_1 K_1(F_1)],\ F_{13} = \frac{1}{[S^2 - M^2]}[\beta_v Kn(1-\eta)E_1\{C_3 I_1(E_1) - C_4 K_1(E_1)\} + \{C_3 I_0(E_1) + C_4 K_0(E_1)\}],$$

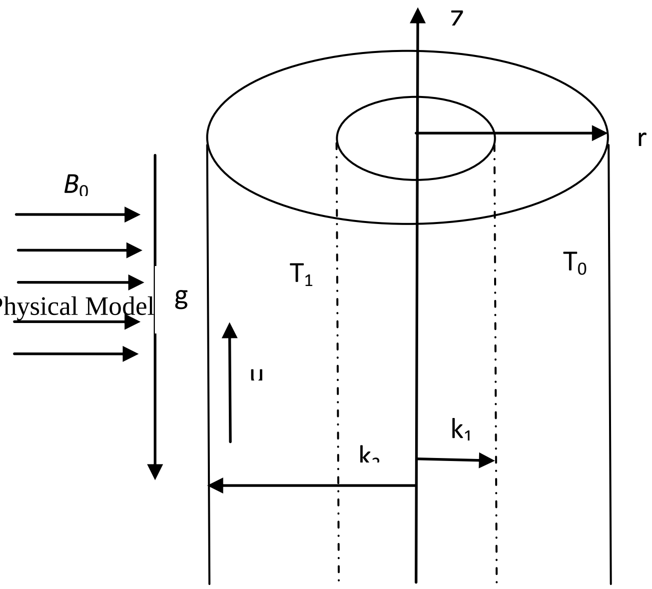

Figure 1. Physical Model

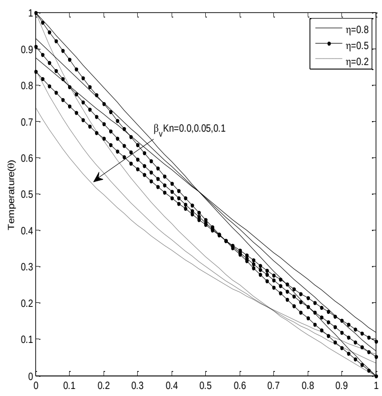

Fig.2,Temperature profile for different values of β_vKn with In=1.64,S=0.5

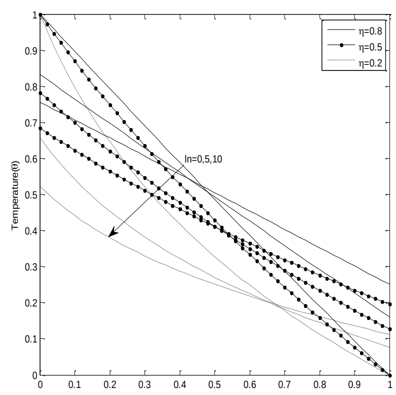

Fig.3,Temperature profile for different values of In with β_vKn=0.05,S=0.5

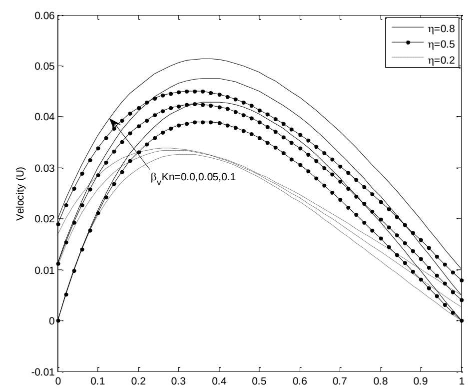

Fig.4,Velocity profile for different values of β_vKn with In=1.64,S=0.5,M=2.0

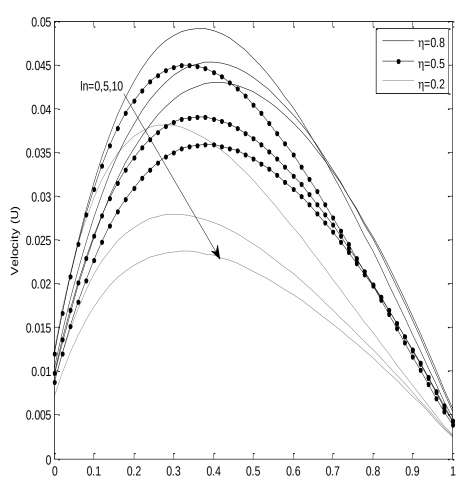

Fig.5,Velocity profile for different values of In with β_vKn=0.05,S=0.5,M=2.0

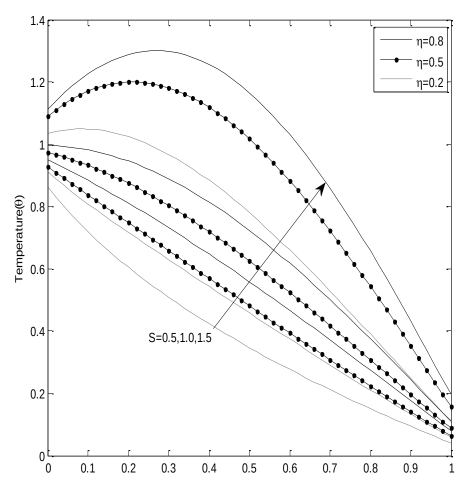

Fig.6a,Temperature profile for different values of S with β_vKn=0.05,In=1.64

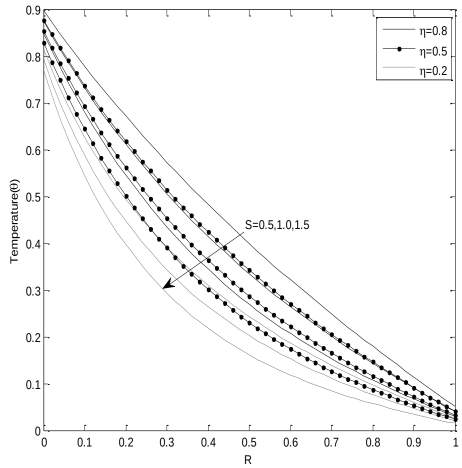

Fig.6b,Temperature profile for different values of S with β_vKn=0.05,In=1.64

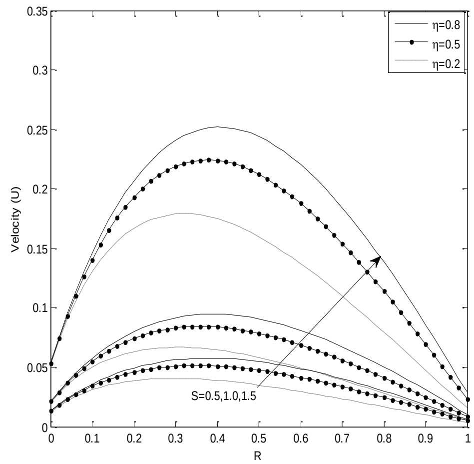

Fig.7a,Velocity profile for different values of S with β_vKn=0.05,In=1.64,M=2.0

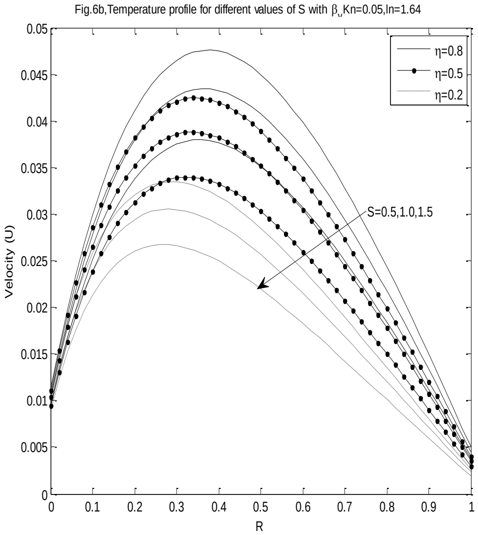

Fig.7b,Velocity profile for different values of S with β_vKn=0.05,In=1.64,M=2.0

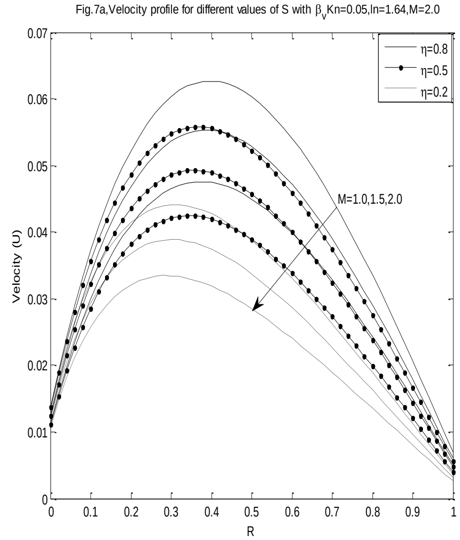

Fig.8,Velocity profile for different values of M with β_vKn=0.05,In=1.64,S=0.5

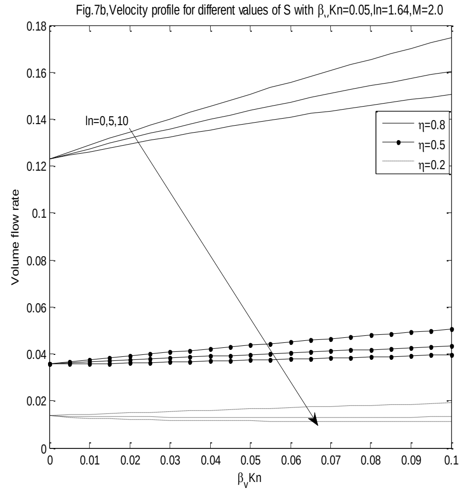

Fig.9,Variation of volume flow rate with β_vKn at different values of In

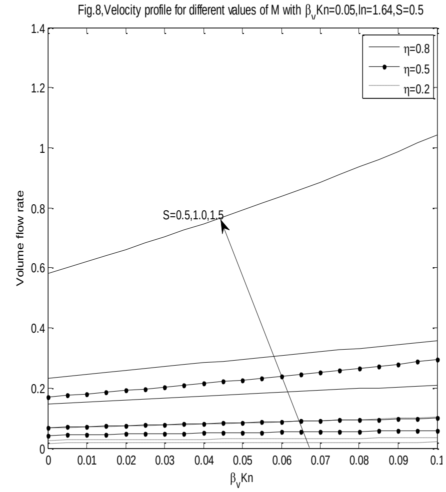

Fig.10a,Variation of volume flow rate with β_vKn at different values of S

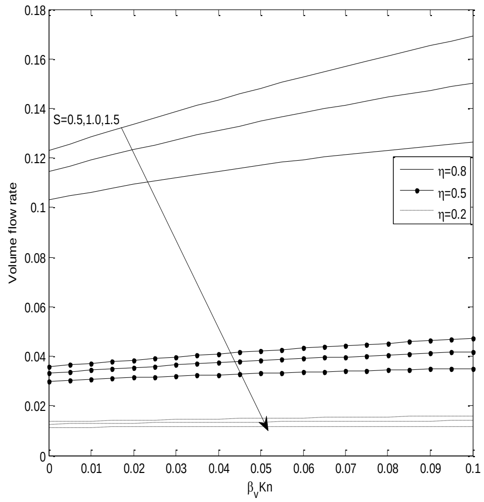

Fig.10b,Variation of volume flow rate with β_vKn at different values of S

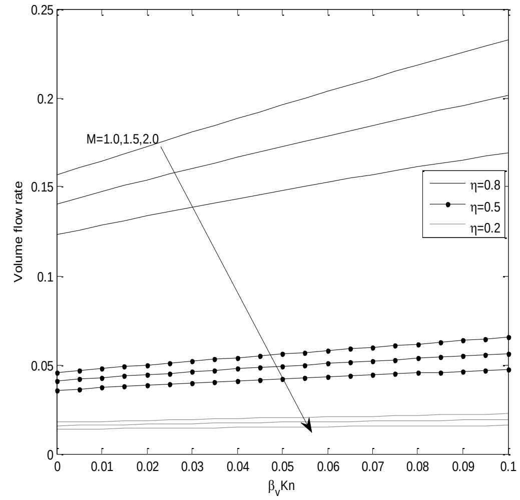

Fig.11,Variation of volume flow rate with β_vKn at different values of M

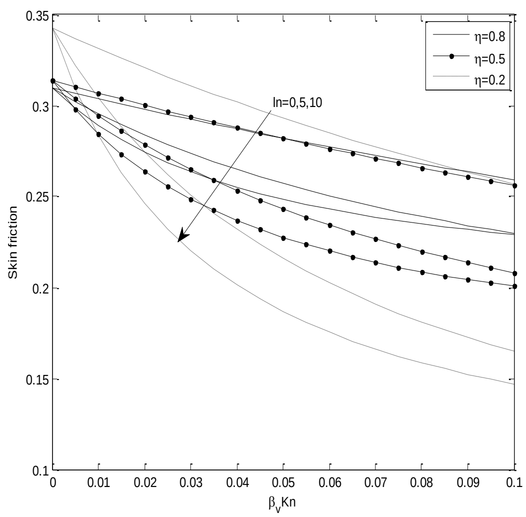

Fig.12,Variation of skin friction on inner cylinder with β_vKn at different values of ln

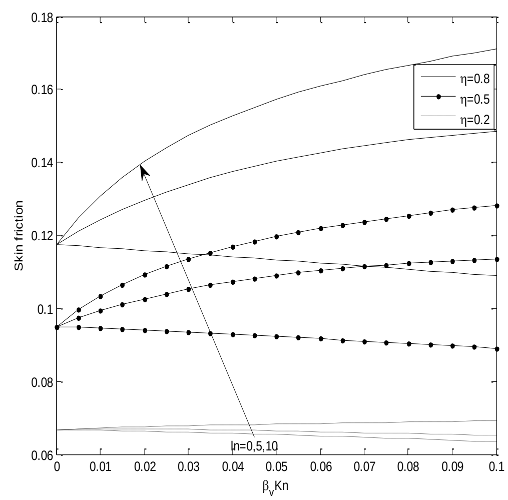

Fig.13,Variation of skin friction on outer cylinder with β_vKn at different values of ln

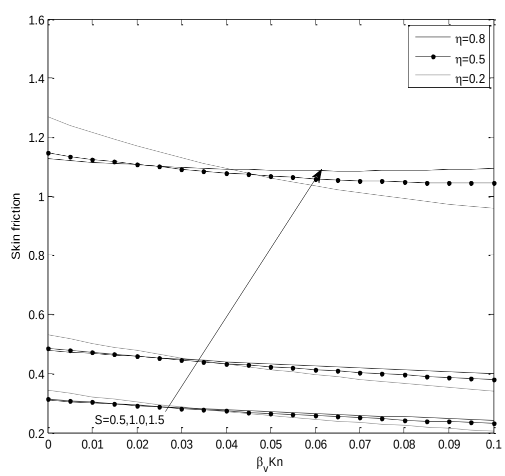

Fig.14a,Variation of skin friction on inner cylinder with β_vKn at different values of S

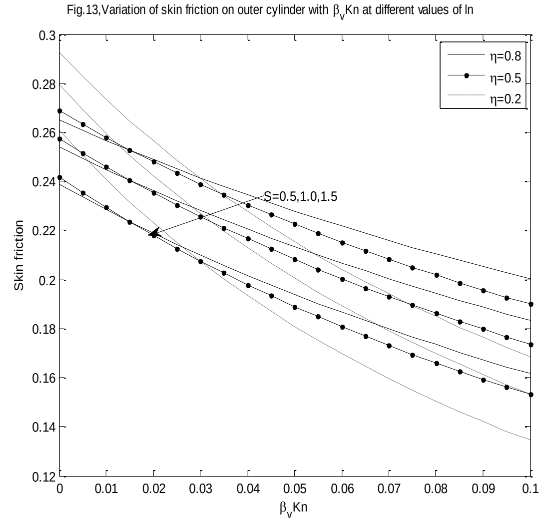

Fig.14b,Variation of skin friction on inner cylinder with β_vKn at different values of S

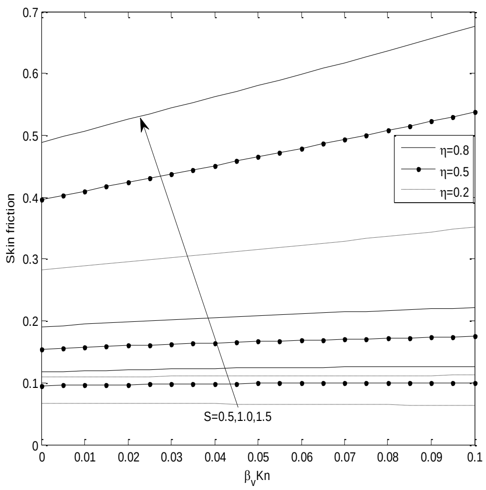

Fig.15a,Variation of skin friction on outer cylinder with β_vKn at different values of S

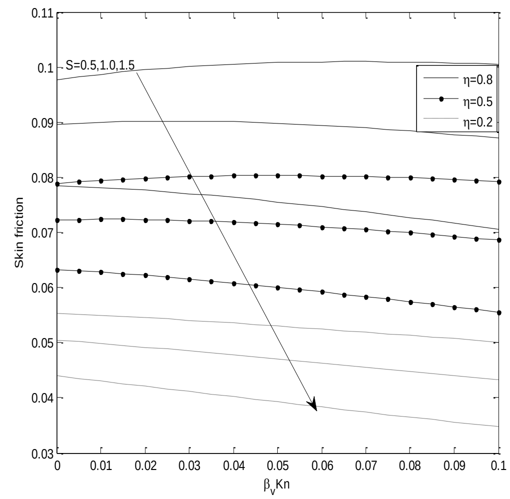

Fig.15b,Variation of skin friction on outer cylinder with β_vKn at different values of S

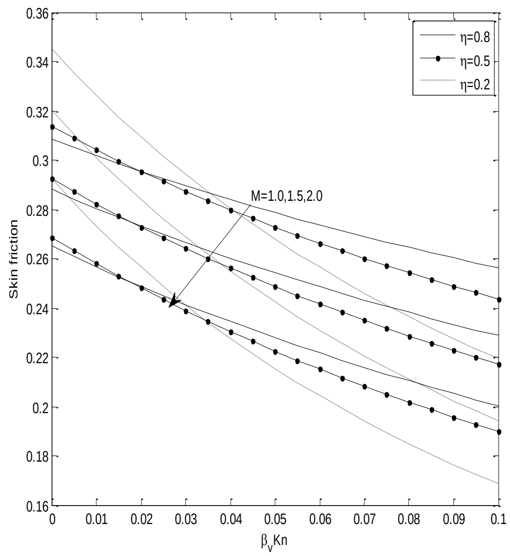

Fig.16,Variation of skin friction on inner cylinder with β_vKn at different values of M

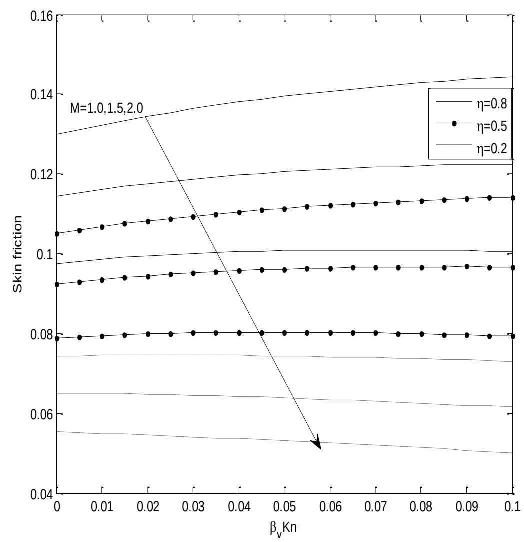

Fig.17,Variation of skin friction on outer cylinder with β_vKn at different values of M

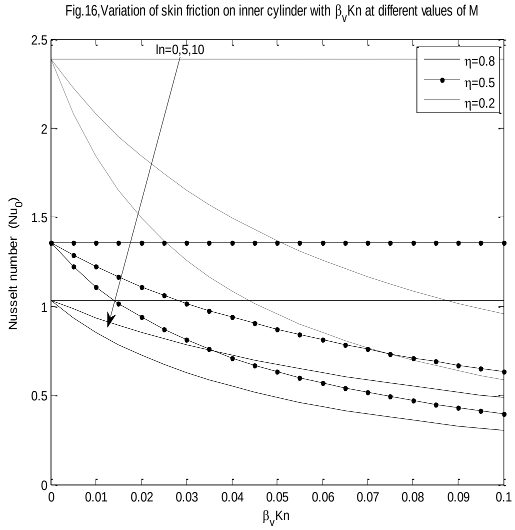

Fig.18,Variation of rate of heat transfer on the inner cylinder versus β_vKn for different values of In

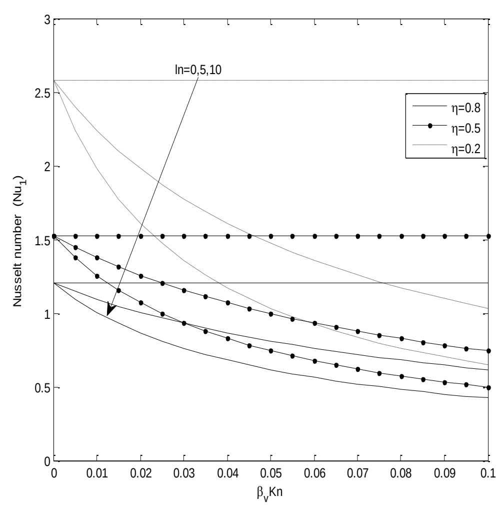

Fig.19,Variation of rate of heat transfer on the outer cylinder versus β_vKn for different values of In

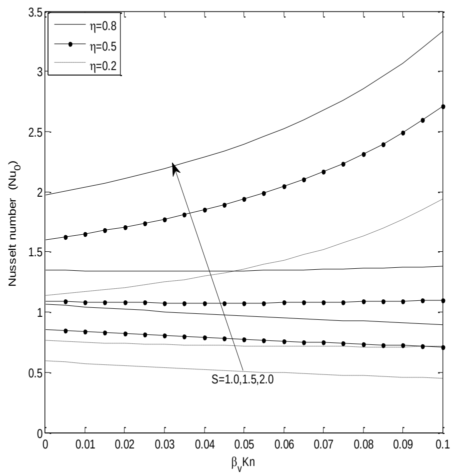

Fig.20a,Variation of rate of heat transfer on the inner cylinder versus β_vKn for different values of S

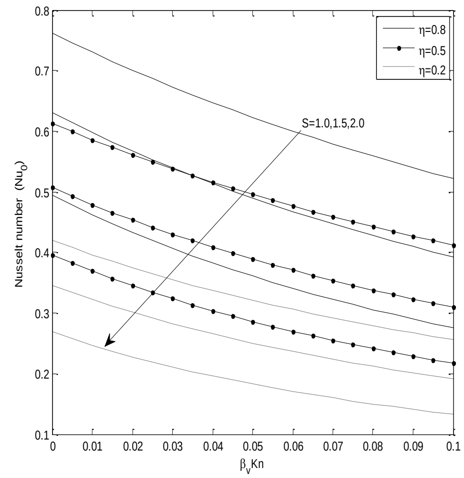

Fig.20b,Variation of rate of heat transfer on the inner cylinder versus β_vKn for different values of S

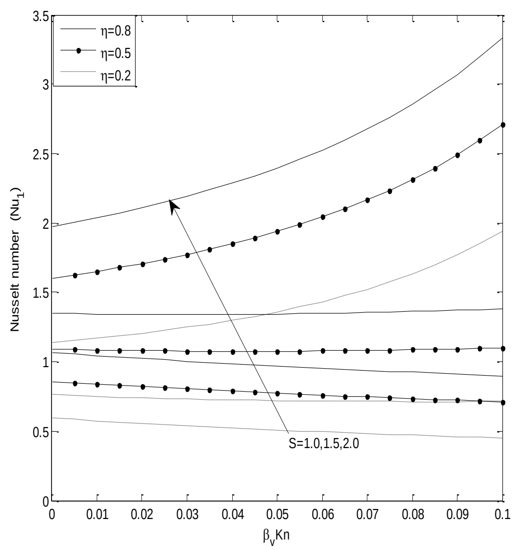

Fig.21a,Variation of rate of heat transfer on the outer cylinder versus β_vKn for different values of S

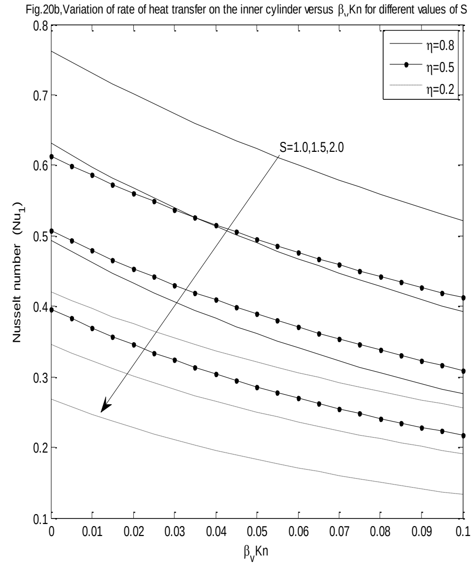

Fig.21b,Variation of rate of heat transfer on the outer cylinder versus β_vKn for different values of S

Table 1: Comparison of the values of velocity obtained in the present work with those obtained by Weng and Chen [9]

		Velocity ($\ln = 1.64$)	
η	R	Weng and Chen [9]	Present work (S and $M \to 0$)
0.2	0.2	0.0527	0.0526
	0.4	0.0537	0.0536
	0.6	0.0431	0.0430
	0.8	0.0269	0.0268
0.5	0.2	0.0651	0.0650
	0.4	0.0730	0.0729
	0.6	0.0624	0.0624
	0.8	0.0408	0.0407
0.8	0.2	0.0712	0.0712
	0.4	0.0838	0.0837
	0.6	0.0745	0.0744
	0.8	0.0504	0.0503

Table 2: Comparison of the values of temperature obtained in the present work with those obtained by Weng and Chen [9]

η	R	Velocity ($\ln = 1.64$)	
		Weng and Chen [9]	Present work ($S \to 0$)
0.2	0.2	0.5428	0.5427
	0.4	0.3592	0.3590
	0.6	0.2253	0.2252
	0.8	0.1198	0.1196
0.5	0.2	0.6761	0.6760
	0.4	0.4873	0.4871
	0.6	0.3236	0.3234
	0.8	0.1793	0.1790
0.8	0.2	0.7335	0.7334
	0.4	0.5547	0.5546
	0.6	0.3837	0.3835
	0.8	0.2200	0.2200

REFERENCES

[1] Chen C.K. and Weng H.C., Natural Convection in a Vertical Microchannel, *J. Heat Transfer*, 2005, 127, pp 1053-1056.

[2] Jha, B. K., Aina, B. and Joseph, S. B., Natural Convection Flow in a Vertical Micro-Channel with Suction/Injection, Journal of Process Mechanical Engineering. 2014, 228 (3), 171-180

[3] Buonomo B., and Manca O., Natural Convection Flow in a Vertical Micro-Channel with Heated at Uniform Heat Flux. Int. J. Therm. Sci. 2012, 49, pp 1333-1344

[4] Buonomo B., and Manca O., Transient Natural Convection Flow in a Vertical Micro-Channel with Heated at Uniform Heat Flux. Int. J. Therm. Sci. 2012, 56, pp 35-47

[5] Khadrawi, A.F, Othman A. and Al-Nimr, M. A., Transient Free Convection Gas Flow in a Vertical Microchannel as described by the Hyperbolic Heat Conduction Model, International J. Thermophysics, 2005; 26(3): 905-918.

[6] Avci M. and Aydin O., Mixed convection in a vertical Microchannel. *ASME J. Heat Transfer*, 2007, 129, pp. 162 – 166.

[7] Avci M. and Aydin O., Mixed convection in a vertical Microannulus between two Concemtric Microtubes. ASME J. Heat Transfer, 2009, 131, pp. 014502 – 4.

[8] Jha B. K. and Aina B., Mathematical Modelling and Exact Solution of Steady Fully Developed Mixed Convection Flow in a Vertical Micro-Porous-Annulus, Journal of Afrika Matematika, 2015, 26, pp 1199-1213

[9] Weng H.C and Chen C.K., Drag Reduction and Heat Transfer Enhancement over a Heated Wall of a Vertical Annular Microchannel. *International journal of heat and mass transfer*, 2009, 52, 1075 - 1079.

[10] Jha, B. K., Aina, Babatunde and Shehu A. M., Combined effects of Suction/Injection and wall surface curvature on Natural Convection Flow in a Vertical Micro-Porous-Annulus, *Journal of Thermophysics and Aerodynamics*, 2015, Vol. 22, 2, pp 217-228

[11] Jha, B. K., Aina, Babatunde and Ajiya A. T., MHD Natural Convection Flow in a Vertical Parallel Plate Microchannel, Ain Shams Engineering Journal, 2015, Vol. 6, pp 289-295.

[12] Jha, B. K., Aina, Babatunde and Ajiya A. T., Role of Suction/Injection on MHD Natural Convection Flow in a Vertical Microchannel, International Journal of Energy & Technology 2015, Vol. 7, pp 30-39.

[13] Jha, B. K., Aina, Babatunde and Sani Isa, Transient Magnetohydrodynamic Free Convective Flow in Vertical Micro-Concentric-Annuli, ProcIMechE Part N: J Nanoengineering and Nanosystems, DOI: 10.1177/1740349915578956

[14] Jha, B. K., Aina, Babatunde and Sani Isa, Fully Developed MHD Natural Convection Flow in a Vertical Annular Microchannel: An exact solution, Journal of King Saud university- Science, 2015, 27, pp 253-259

[15] Jha, B. K., and Babatunde Aina, MHD Natural Convection Flow in a Vertical Micro-Porous- Annulus in the Presence of Radial Magnetic Field, *Journal of Nanofluids*, 2016, doi:10.1166/jon.2016.1204

[16] Jha, B. K., Babatunde Aina and Sani Isa, MHD Natural Convection flow in a Vertical Micro-Concentric-Annuli in the Presence of Radial Magnetic Field: An Exact Solution, *Journal of Ain Shams Engineering*, 2016, 7, pp 1061-1068

[17] Sheikholeslamia M., Gorji-Bandpy M., Ganji D. D., Rana P., and Soheil Soleimani, Magnetohydrodynamic free convection of Al2O3–water nanofluid considering Thermophoresis and Brownian motion effects, *Computers and Fluid*, 2014, 94, pp 147-160.

[18] Khan I. and Ellahi R., Some unsteady MHD flows of a second grade fluid through porous medium, Journal Porous Media (ISI Indexed, I.F 0.684), 2008, 11(4), 389-400

[19] Farhad A., Norzieha M., SSharidan S., Khan I. and Samiuthaq, On Hydromagnetic Rotating Flow in a Porous Medium with Slip Condition and Hall Current, International Journal of the Physical Sciences, 2012, 7(10), pp. 1540-1548.

[20] Jha B. K., Transient Free Convective Flow in a Vertical Channel with Heat Sinks, Int. J. Appl. Mech. Eng, 2001, 6 (2), pp.279–28

[21] McKenzie D.P., Roberts J.M. and Weiss N.O., Convection in the Earth's Mantle: Towards a Numerical Simulation, J. Fluid Mech, 1974, 62, pp.465–538.

[22] Crepeau J.C. and Clarksean R., Similarity Solutions of Natural Convection with Internal Heat Generation, ASME J. Heat Transfer 119 (1997) 183–185.

[23] Baker I., Faw R.E. and Kulacki F.A., Post-Accident Heat Removal Part I: Heat Transfer within an Internally Heated non Boiling Liquid Layer, Nucl. Sci. Eng, 1976, 61, pp.222–230

[24] Delichatsios M.A. Air Entrainment into Buoyant Jet Flames and Pool Fires, In: P.J. DiNenno, *et al*., (Eds.), The SFPA Handbook of Fire Protection Engineering, NFPA Publications, Quincy, MA, 1988, pp.306–314.

[25] Westphal B.R., Keiser D.D., Rigg R.H., and Laug D.V., Production of Metal Waste Forms from Spent Nuclear Fuel Treatment, DOE Spent Nuclear Fuel Conference, Salt Lake City, UT, 1994, pp. 288–294

[26] Chamkha A. J., Non-Darcy fully developed mixed convection in a porous medium channel with heat generation/absorption and hydromagnetic effects, Numerical Heat Transfer, Part A, 1997, 32, 653-675

[27] R.M. Inman, Experimental study of temperature distribution in laminar tube flow of a fluid with internal heat generation, Int. J. Heat Mass Transfer, 1962, 5, 1053

[28] Ostrach S., Laminar Natural Convection Flow and Heat Transfer of Fluids with and without Heat Sources in Channels with Constant wall Temperatures, NACA TN, 1952, pp 2863

[29] Low G. M., Stability of Compressible Laminar Boundary Layer with Internal Heat Sources or Sinks, J. Aero. Sci., 1955, 22, 329

[30] Chambre P. L., Laminar Boundary Layer with Distributed Heat sources or Sinks, Appl. Sci. Res. Sec. A., 1957, 6, 393

[31] Toor H. L., Heat Transfer in Forced Convection with Internal Heat Generation, J. Am. Inst. Chem. Eng. 1958, 4, 319

[32] Gee R. E. and Lyon J. B., Non Isothermal Flow of Viscous Non-Newtonian Fluids, Ind. Eng. Chem., 1957, 49, 956.

[33] Modejski J., Temperature Distribution in Channel Flow with Friction, Int. J. Heat Mass Transfer, Vol. 6, 919630, pp 49.

[34] Toor H. L., The energy equation for viscousflow, Ind. Eng. Chem. 48 (1956) 922

[35] Moalem D., Steady state heat transfer with porous medium with temperature dependent heat generation, Int. J. Heat Mass Transfer, 1976, 19, 529.

[36] Foraboschi F. P. and Federico I. D., Heat Transfer in Laminar Flow of Non-Newtonian Heat Generating Fluids, Int. J. Heat Mass Transfer, 1964, 7, 315

[37] Basant K. Jha, Michanel Oni and Babatunde Aina, Steady Fully Developed Mixed Convection Flow in a VerticalMicro-Concentric-Annulus with Heat Generating/AbsorbingFluid: An Exact Solution, *Journal of Ain Shams Engineering*, 2016, DOI:10.1016/j.asej.2016.08.005

[38] Crammer, K. R. and Pai, S., Magnetohydrodynamics for Engineers and Applied Physicist. McGraw Hill Book Company, New York, 1973

[39] Arpaci, V.S., 1966. Conduction Heat Transfer. Addison Wesley, Reading, MA, pp. 135–136.